

Advances in Chip-Scale Atomic Frequency References at NIST

S. Knappe*^a, V. Shah^b, A. Brannon^c, V. Gerginov^d, H.G. Robinson^a, Z. Popović^c,
L. Hollberg^a, J. Kitching^a

^aTime and Frequency Division, NIST, Boulder, CO 80305[†];

^bDepartment of Physics, The University of Colorado, Boulder, CO 80309;

^cDept. of Elec. and Comp. Engineering, The University of Colorado, Boulder, CO 80309;

^dDepartment of Physics, The University of Notre Dame, Notre Dame, IN 46556

ABSTRACT

Coherent population trapping (CPT) resonances usually exhibit contrasts below 10 % when interrogated with frequency modulated lasers. We discuss a relatively simple way to increase the resonance contrast to nearly 100 % generating an additional light field through a nonlinear four-wave mixing interaction in the atomic vapor¹. A similar method can also be used to create a beat signal at the CPT resonance frequency that can injection-lock a low-power microwave oscillator at 3.4 GHz directly to the atomic resonance². This could lead to chip-scale atomic clocks (CSACs) with improved performance. Furthermore, we introduce a miniature microfabricated saturated absorption spectrometer³ that produces a signal for locking a laser frequency to optical transitions in alkali atoms. The Rb absorption spectra are comparable to signals obtained with standard table-top setups, although the rubidium vapor cell has an interior volume of only 1 mm³ and the volume of the entire spectrometer is around 0.1 cm³.

Keywords: chip-scale atomic clock, CSAC, frequency reference, microfabrication, saturation spectroscopy

1. INTRODUCTION

Since the proposal of microelectromechanical systems (MEMS) atomic frequency references⁴, much progress has been made towards the development of commercial devices⁵. The development of MEMS vapor cells⁶ and suitable laser technologies⁷ have been important milestones on the route to chip-scale atomic clock (CSAC) physics packages⁸ with size 10 mm³ and frequency stabilities below $5 \times 10^{-11}/\tau^{1/2}$. The power consumption of physics packages has been reduced to below 10 mW at room temperature⁹. With these specifications, CSACs could have a broad range of civil¹⁰ and military¹¹ applications, such as global navigation satellite systems (GNSS) with improved performance, and secure communication systems. Recently, full CSAC packages of size 100 cm³, power consumptions around 150 mW, and frequency stabilities near $5 \times 10^{-10}/\tau^{1/2}$ have been demonstrated as prototypes¹². Here, the physics packages have been implemented with a low-power local oscillator (LO) with power consumptions below 10 mW¹³ and control electronics. Activities to miniaturize these devices even further to volumes of 1 cm³ with power consumptions of 50 mW are well underway¹⁴.

Such devices are usually passive frequency references that require microwave oscillators as a modulation source. The oscillators are then locked to the atomic resonance. A standard way of doing this is modulating the output frequency of the LO at a few kilohertz and using phase sensitive detection of the atomic resonance. Therefore, the clock signal has a second slow modulation superimposed. Furthermore, locking range and correction bandwidth are limited in this technique. The stringent requirements on tunability and drift place further challenges for the design of these oscillators. In this paper, we demonstrate a simple and robust way to stabilize a low-power LO to the atomic resonance by self-injection locking. This results in improved phase noise and short-term frequency stability of the CSAC.

*knappe@boulder.nist.gov; phone 1 303 497-3334; fax 1 303 497-7845; <http://tf.nist.gov/ofm/smallclock/index.htm>

[†] Contribution of NIST an agency of the U.S. government; not subject to copyright.

Most CSACs are based on coherent population trapping¹⁵ (CPT), where a so-called coherent dark state is populated in the ground states of alkali atoms by interrogation with a bichromatic light field. If the light is resonant with the D line of the atoms and the beat frequency between two light fields equals the one of the ground-state hyperfine splitting, the absorption of light by the atoms is reduced. These resonances can have Q-factors of greater than 1 million, even in cells with volumes of 1 mm³. Many of their properties are similar to those of conventional microwave double resonances, but they are usually detected with transmission contrasts below 10 %. In this paper, we present a method to increase this contrast to more than 90 %¹.

2. HIGH CONTRAST CPT RESONANCES

The intrinsically low contrast of the CPT resonances has been of concern. On the D2 line, contrasts have been limited to below 1 % and on the D1 line to about 25 %¹⁶, mostly due to the multilevel energy structure of the atoms. Several techniques for increasing this contrast have been developed¹⁷. Most of these achieve higher contrasts, but at the expense of broader resonance lines. In most CSACs, nonresonant modulation sidebands are present in the detected light and reduce the contrast even further. Figure 1 shows a typical CPT transmission spectrum of the D1 line of ⁸⁷Rb vapor. Three CPT resonances are visible when circularly polarized light is used in a longitudinal magnetic field. They correspond to transitions between ground states with equal magnetic quantum number and the frequency of the central 0-0 “clock transition” is insensitive to magnetic fields in first order. It can be seen that the transmission contrast (A/B) is only several percent, limited by a large background. This background light is the major contributor to photon shot noise, amplitude, and frequency noise, converted into power fluctuations through the atomic resonance¹⁸. We demonstrate here a method that eliminates nearly all background light and creates a signal on the photodetector only, when the CPT condition is fulfilled. A pump laser is modulated to create a ground-state coherence in the atoms under CPT condition. When a monochromatic probe laser is added, a conjugate light field can be created through a four-wave mixing process¹⁹ in the atoms. The light from pump and probe laser is eliminated by spectral and polarization filtering, and only the conjugate light field is detected against nearly no light background.

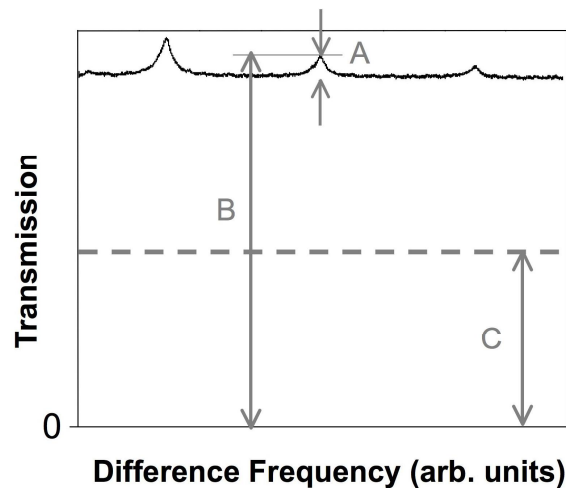


Fig. 1. CPT transmission spectrum of the D1 line of ⁸⁷Rb vapor in a longitudinal magnetic field. The center resonance corresponds to the 0-0 “clock transition”. The off-resonant modulation sidebands cause a background labeled C. The transmission contrast is defined as A/B.

Such an experiment was performed in ⁸⁷Rb vapor. A right-hand circularly polarized pump laser was modulated at 3.417 GHz, half the ground-state splitting frequency of ⁸⁷Rb (see Fig. 2a). It was tuned such that the two first-order modulation sidebands were resonant with the transitions $|F=1, m_f\rangle \rightarrow |F', m_f+1\rangle$ and $|F=2, m_f\rangle \rightarrow |F', m_f+1\rangle$ to create a two-photon CPT resonance. The probe laser was left-hand circularly polarized and resonant with the $|F=2, m_f\rangle \rightarrow |F', m_f-1\rangle$ transition. Both fields are in the same spatial mode,

combined in the experiment on a polarizing beamsplitter (see Fig. 2b). Pump and probe laser had peak intensities of 6.2 mW/cm^2 and 1.16 mW/cm^2 , respectively. Through the four-wave mixing process, a conjugate light field is spontaneously generated in the same polarization mode as the probe field. After passing through the ^{87}Rb vapor cell containing a mixture of nitrogen and argon at 6.6 kPa inside a magnetic shield, the pump beam is eliminated with the combination of a quarter waveplate and a polarizer. The cell was heated such that 96 % of the pump light was absorbed when detuned from two-photon resonance. Afterwards, the probe laser field is absorbed by an optically dense ^{85}Rb filter cell. The conjugate light field, attenuated by only 5 % by the filter cell, is then detected with a DC photodetector. Figure 3 shows a resonance detected in this way as the modulation frequency of the pump laser is scanned across the atomic two-photon resonance. The contrast, in this case defined as the ratio of the CPT amplitude to the total light on resonance, was measured to be 90.3 %. It was limited by the 3 nW of leakage light that reached the photodetector as a result of a secondary spectral laser mode of the probe laser and that was detuned from the primary mode by roughly 2 GHz. When a longitudinal magnetic field is applied, three resonances can be detected with nearly equal contrast but somewhat lower amplitude.

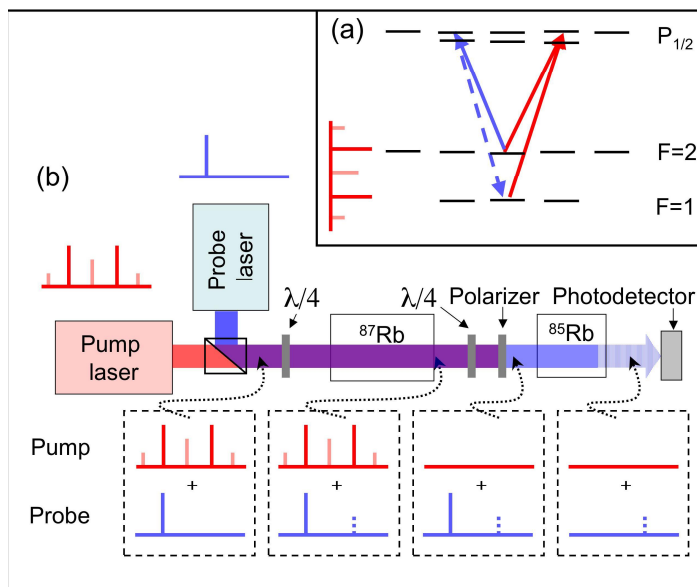


Fig. 2. (a) Diagram of the relevant energy levels in ^{87}Rb . The pump laser is resonant with the transition drawn in red, the probe laser with the one indicated by the solid blue line. The four-wave mixing process creates a conjugate light field denoted by the dashed blue line. (b) Experimental setup used to observe the conjugate light field against nearly zero light background.

For the application to chip-scale clocks or magnetometers²⁰, the benefit of high resonance contrast is partially offset by a lower signal amplitude due to a finite conversion efficiency of the four-wave mixing process. Under optimal conditions, contrasts up to 15 % can be reached in a conventional CPT setup, so that this technique yields an improvement by a factor of six. Resonance linewidths were roughly equal in both cases. The average power generated in the conjugate light field was roughly 12 % of the transmitted power change in a conventional CPT setup. Therefore, the improvement when using this technique in a completely optimized, photon shot-noise-limited system is expected to be small. For many applications though, especially in CSACs, optimal conditions are difficult to obtain. Typical operating resonance contrasts in MEMS cells containing high buffer gas pressures are a few percent (and rather 0.1 % for the D2 line). In these cases, the improvements are expected to be much more significant. Another problem in CSACs arises from the frequency noise of the laser. In order to achieve good modulation efficiency at frequencies of several gigahertz, low-power consumption vertical-cavity surface-emitting lasers (VCSELs) have been used. Optimal modulation efficiency, i.e., maximum optical power in the first-order sidebands, has been achieved with -6 dBm modulation power at 3.4 GHz in some VCSELs. The VCSELs used here have linewidths wider than 50 MHz and considerable frequency noise. VCSELs with less FM noise have

been found often to yield much lower modulation efficiencies. Therefore, the stability of the CSAC could be improved by using a VCSEL that can be readily modulated as the pump laser, at the expense of higher frequency noise, and a low-noise VCSEL, with worse modulation efficiency, as the probe laser. Since first experiments indicate that the FM noise from the pump laser is not transferred to the conjugate light field, a substantial amount of FM noise could be eliminated. Finally, apart from applications such as atomic clocks and magnetometers, this technique could be attractive for areas such as slow light with electrically induced transparency (EIT) and quantum memory²¹.

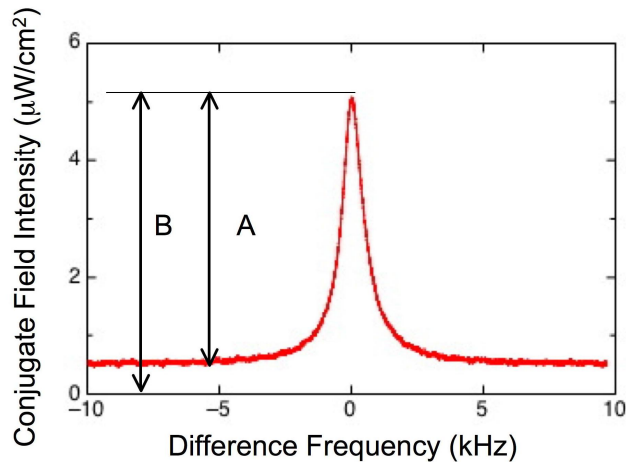


Fig. 3. Conjugate light field power as a function of detuning from the two-photon resonance (6.834 GHz). Contrast in this case is defined as A/B . The residual light ($B-A$) is due to a secondary spectral mode of the probe laser.

3. SELF-INJECTION LOCKED LOCAL OSCILLATOR

Most CSACs are currently passive frequency references that lock a local oscillator to an atomic resonance. In the case of CPT, the LO is used as a modulation source to directly modulate the injection current of the VCSEL. It is then stabilized to the atomic resonance by use of phase sensitive-detection, where the LO is modulated at a few kilohertz and the photodetector signal is demodulated in phase with this modulation. A fairly small locking range and correction bandwidth often limit the performance of these passive clocks. The LO must have a small frequency drift and large tuning range, while simultaneously exhibiting good short term stability and the ability to fine-tune the frequency. This places stringent constraints on the design of the LO, apart from low power consumption and small size. As a result, the LO can limit the performance of the CSAC, especially the LO phase noise at twice the modulation frequency²². Furthermore, it is often desired that the output signal of the clock does not contain modulation sidebands. In standard passive systems, these sidebands are removed with the use of another oscillator and a phase-lock loop.

As an alternative, an active clock scheme could eliminate the LO altogether. In the case of a Raman oscillator, for example, the laser is modulated by use of the beat signal that is generated on the fast photodetector at the ground-state hyperfine frequency²³. These systems can be difficult to lock and often require fairly high laser intensities, because of resonance contrasts below 10 %. Furthermore, phase shifts in the oscillating loop can be difficult to control. In the previous section, resonances with very high contrasts were demonstrated, enabling a robust and fast lock of a low-power LO to the CPT resonance. Here, the four-wave mixing signal can be used to injection lock a low-power LO² to the beat frequency generated on the fast photodiode, resulting in a much wider locking bandwidth and improved clock stability.

In this system, which is similar to the previous setup, a VCSEL is modulated at half the ground-state splitting frequency by a 3.417 GHz local oscillator. The VCSEL is tuned to the D1 line of ⁸⁷Rb such that the two first-order sidebands are in resonance with the transition from the two hyperfine ground states

creating a CPT resonance in the atomic vapor cell. A monochromatic probe laser is added with the opposite circular polarization, as shown in Figure 4. The phase conjugate signal is generated in the atoms with the same polarization as the probe laser, separated in frequency by 6.834 GHz. Again, the pump light is eliminated by the combination of a quarter waveplate and a polarizer. However, unlike the DC detection method, both the transmitted probe light and the conjugate light are detected with a fast photodetector, yielding a beat signal at 6.834 GHz with microwave power at -90 dBm. After 20 to 50 dB amplification, the signal is directly inserted into the output of the LO. Since the microwave signal is injection locked at the second harmonic, no additional frequency conversion is required. Furthermore, the LO can operate at half the hyperfine splitting frequency, eliminating the need to shield the vapor cell from radiated power at the fundamental hyperfine frequency. Such a radiated RF field at the location of the atoms can cause direct microwave transitions between the hyperfine ground states and destroy the CPT resonance.

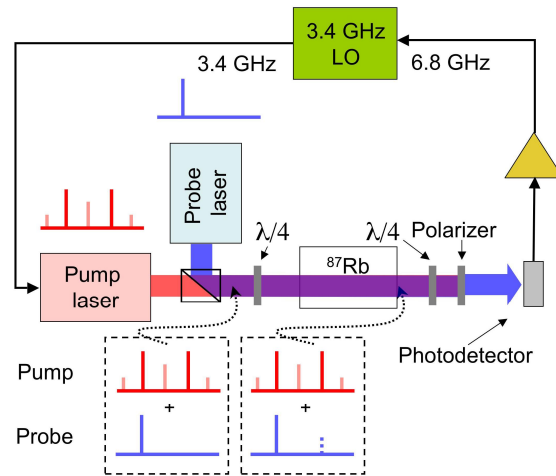


Fig. 4. Experimental setup to injection-lock the local oscillator to the four-wave mixing signal.

A comparison of the conventional passive lock with the injection lock using the four-wave mixing signal can be found in Figure 5. The single-sideband phase noise of the free-running LO at 3.417 GHz, developed for a CSAC, is shown in green. When passively locked to the CPT resonance in the conventional way, the phase noise at a 1 Hz offset is improved by 40 dB (red trace in Fig. 5). The servo bump near the locking bandwidth of 1 kHz and spike at the modulation frequency of 3.49 kHz can be clearly seen. As expected, the phase noise equals that of the free-running LO at frequencies outside the locking bandwidth. Locking bandwidths larger than a few kilohertz were difficult to achieve with small, low-power CSAC control electronics, so CSACs were limited mostly to these bandwidths.

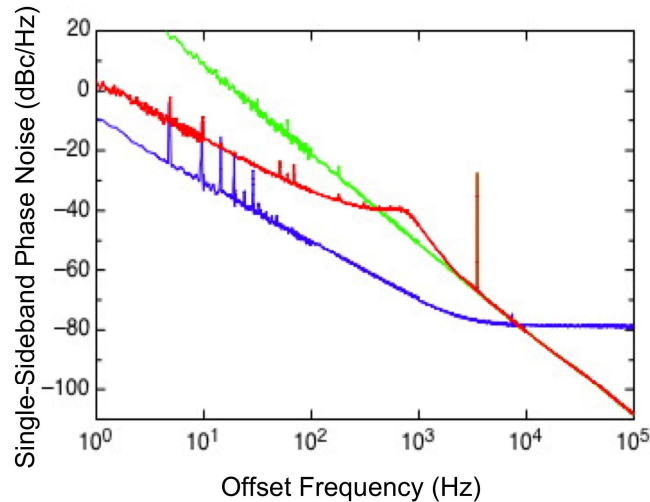


Fig. 5. Phase noise plots comparing the unlocked LO (green) to typical passive servo control (red) and to the injection-locking method (blue).

The LO was injection-locked to the four-wave mixing signal, as described previously, keeping the laser intensities and the LO output the same as in the passively locked case. This method eliminated both the need for additional modulation and the lock-in amplifier. The blue trace in Figure 5 shows the phase noise obtained in this case; it achieves a 10 dB improvement over the passive lock at 1 Hz offset and 30 dB at 1 kHz offset. Around -79 dBc/Hz, it is limited by the fact that the LO injection locks itself to the noise from the photodiode amplifier. The noise finally rolls off at frequencies larger than the injection-locking bandwidth of 20 MHz, although this depends on the power of the 6.8 GHz signals inserted into the LO. Lower power will reduce the phase noise but will also reduce the bandwidth. The high bandwidth of the lock should make it much easier to keep the CSAC locked during fast perturbations and over large frequency drifts.

4. MEMS SATURATED ABSORPTION SPECTROMETER

Until now, all chip-scale frequency references have been based on microwave transitions. Many laser spectroscopy experiments, however, need lasers stabilized to a narrow optical transition in atoms. For this, sub-Doppler spectroscopy of transitions in alkali atoms has become a widely used tool for many atomic physics experiments²⁴. Here, a miniature saturated absorption spectrometer is presented with a volume of less than 0.1 cm³ and with a performance that is projected to be similar to that of table-top setups³. By locking a single-mode diode laser to a transition in cesium or rubidium, a stable optical frequency at 852 nm, 895 nm, 780 nm, or 795 nm could be maintained. Furthermore, the setup could easily be extended to potassium or iodine. Finally, by adding a periodically poled lithium niobate (PPLN) waveguide in front of the spectrometer, such a device could be used to stabilize telecom lasers between 1540 nm and 1560 nm.

In this spectrometer, the vapor cell of 1 mm³ interior volume contained rubidium. It was fabricated in a way similar to that used for CSACs²⁵. The major difference was that CSAC cells usually require buffer gasses, while in the case of the spectrometer much care had to be taken to eliminate any additional gasses that might be present inside the cell cavity. Such gasses would homogeneously broaden the excited state of the alkali atoms and therefore broaden the saturation Lamb dip. For this purpose the cell body and windows were baked extensively, and additionally, a getter was placed inside the cell cavity. The cell was heated to ~45 °C with two transparent indium tin oxide (ITO) heaters placed on both windows of the cell. Due to the much faster diffusion of the alkali atoms inside the cell when no buffer gas is present, more care had to be taken to keep the windows at slightly higher temperatures than the cell body.

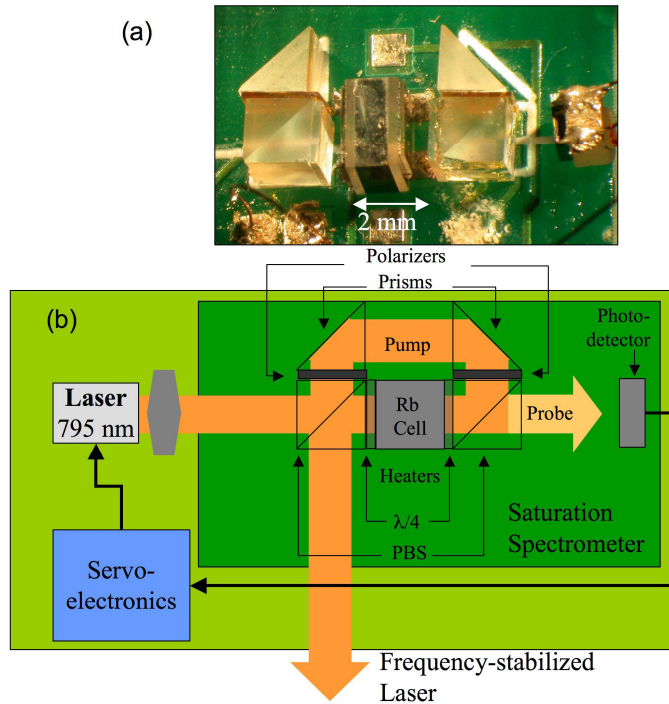


Fig. 6. (a) Photograph of the microfabricated saturated absorption spectrometer. (b) Schematic of microfabricated setup, which consists of a vapor cell with two heaters, two polarizing beam splitters, two prisms, two quarter waveplates, and a photodetector. The laser and the control electronics are not shown in the photo, but could be located very close to the tiny spectrometer.

Vapor cell and heaters were then glued onto a PC board, and contact to the solder pads on the board was made with indium solder. A photograph and schematic of the system can be seen in Figure 6. Two polarizing beamsplitters of size 2 mm separated the pump and probe beams. Two quarter-wave plates created circularly polarized light inside the vapor cell. Two additional polarizers were used to further clean up the polarizations, and microprisms reflected the beam. All micro-optical components were commercially available and had planar surfaces for ease of alignment. A photodiode with a 1 mm diameter active area collected the transmitted light of the probe beam.

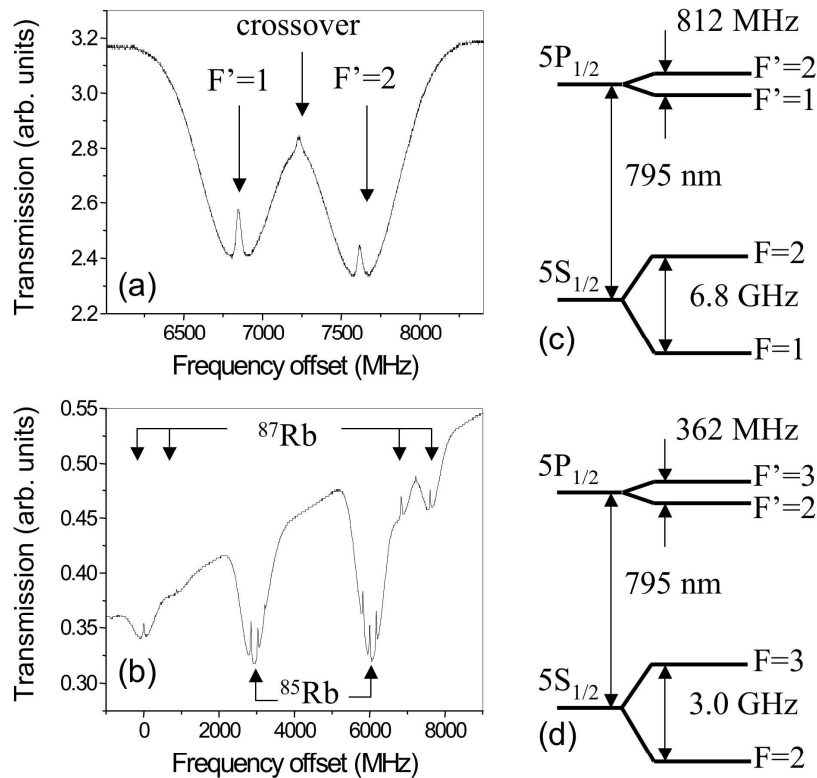


Fig. 7. (a) Spectrum of the transitions $5S_{1/2}, F=2 \rightarrow 5P_{1/2}, F'=1$ and 2 in isotopically enriched ^{87}Rb measured with the microfabricated saturation spectrometer. (b) Saturated absorption spectrum of all D1-line transitions in natural Rb, measured in a microfabricated vapor cell of interior volume 1mm^3 . (c) Relevant energy level structure of ^{87}Rb . (d) Relevant energy level structure of ^{85}Rb .

Light from a distributed Bragg reflector (DBR) laser at 795 nm wavelength was used to measure a saturated absorption spectrum in the setup just described. Such a spectrum can be seen in Figure 7 (a and b). The two center peaks of Figure 7b correspond to the transitions in ^{85}Rb , the four outer resonances correspond to ^{87}Rb . The Lamb dips can be seen for all transitions, and cross-over resonances are clearly visible. Linewidths and contrasts of the resonances are comparable to those measured in larger tabletop systems. The smaller diameter of the laser beam reduces the power on the atoms probed, however, and therefore reduces the signal-to-noise ratio for constant intensity. Nevertheless, some simple estimates predict that the frequency instability of a diode laser locked to a transition in such a MEMS spectrometer will most likely be limited by other systematic uncertainties, and that a long-term frequency instability below 100 kHz should be possible.

5. CONCLUSIONS

A relatively simple way to increase the resonance contrast to nearly 100 % was discussed, based on the generation of an additional light field through a nonlinear four-wave mixing interaction in the atomic vapor. A similar method was also used to create a beat signal at the CPT resonance frequency that can injection-lock a low-power microwave oscillator at 3.4 GHz directly to the atomic resonance. This could

lead to chip-scale atomic clocks (CSACs) with improved performance. A miniature microfabricated saturated absorption spectroscopy setup was introduced. It produces a signal for locking a laser frequency to optical transitions in alkali atoms. The Rb absorption spectra are comparable to signals obtained with standard table-top setups, although the rubidium vapor cell has an interior volume of only 1 mm^3 and the volume of the entire spectrometer is around 0.1 cm^3 .

REFERENCES

Portions of this manuscript have been published before in references 1, 2, and 3.

1. V. Shah, S. Knappe, L. Hollberg, and J. Kitching, "Generation of coherent population trapping resonances with nearly 100% transmission contrast," *Opt. Lett.*, accepted (2007).
2. A. Brannon, V. Shah, Z. Popović, V. Gerginov, S. Knappe, L. Hollberg, and J. Kitching, "Self-Injection Locking of a Low-Power Microwave Oscillator by Using 4-wave Mixing in an Atomic Vapor," European Frequency and Time Forum (EFTF) joint with IEEE Frequency Control Symposium (FCS), Geneva, Switzerland, 2007.
3. S. Knappe, H.G. Robinson, and L. Hollberg, "Microfabricated Saturated Absorption Spectroscopy with Alkali Atoms," *Opt. Expr.* **15** (10), 6293-6299 (2007).
4. J. Kitching, S. Knappe, and L. Hollberg, "Miniature vapor-cell atomic-frequency references," *Appl. Phys. Lett.* **81** (3), 553-555 (2002).
5. D. Carlson QD. Youngner, L. Lust, S. Lu, L. Forner, H. Chanhvongsak, T. Stark, "A manufacturable chip-scale atomic clock," *Transducers & Eurosensors*, Lyon, France, 2007; R. Lutwak, P. Vlitaz, M. Varghese, M. Mescher, D. K. Serkland, and G. M. Peake, "The MAC - A Miniature Atomic Clock," Joint Meeting of the IEEE International Frequency Control Symposium and the Precise Time and Time Interval (PTTI) Systems and Applications Meeting, Vancouver, Canada, 2005.
6. L. A. Liew, S. Knappe, J. Moreland, H. Robinson, L. Hollberg, and J. Kitching, "Microfabricated alkali atom vapor cells," *Appl. Phys. Lett.* **84** (14), 2694-2696 (2004).
7. D. K. Serkland, G. M. Peake, K. M. Geib, R. Lutwak, R. Michael Garvey, M. Varghese, and M. Mescher, "VCSELs for atomic clocks," *Proceedings of SPIE - The International Society for Optical Engineering*, 2006.
8. S. Knappe, V. Shah, P. D. D. Schwindt, L. Hollberg, J. Kitching, L. A. Liew, and J. Moreland, "A microfabricated atomic clock," *Appl. Phys. Lett.* **85** (9), 1460-1462 (2004); S. Knappe, P. D. D. Schwindt, V. Shah, L. Hollberg, J. Kitching, L. Liew, and J. Moreland, "A chip-scale atomic clock based on Rb-87 with improved frequency stability," *Opt. Expr.* **13** (4), 1249-1253 (2005).
9. R. Lutwak, J. Deng, W. Riley, M. Varghese, J. Leblanc, G. Tepolt, M. Mescher, D. K. Serkland, K. M. Geib, and G. M. Peake, "The chip-scale atomic clock - low-power physics package," 36th Annual Precise Time and Time Interval (PTTI) Meeting, Washington, DC, 2004.
10. J. A. Kusters and C. A. Adams, "Performance requirements of communication base station time standards," *RF Design*, May, 28-38 (1999).
11. J. R. Vig, "Military applications of high accuracy frequency standards and clocks," *IEEE Trans. UFFC* **40** (5), 522-527 (1993).
12. R. Lutwak, A. Rashed, M. Varghese, G. Tepolt, J. Leblanc, M. Mescher, D. Serkland, and G. Peake, "The Miniature Atomic Clock - Pre-Production Results," European Frequency and Time Forum (EFTF) joint with IEEE Frequency Control Symposium (FCS), Geneva, Switzerland, 2007.

13. A. Brannon, M. Janković, J. Breitbarth, Z. Popović, V. Gerginov, V. Shah, S. Knappe, L. Hollberg, and J. Kitching, "A Local Oscillator for Chip-Scale Atomic Clocks at NIST," IEEE Freq. Control Symp., Miami, FL, 2006.
14. D. Youngner, L. Lust, D. Carlson, S. Lu, L. Forner, H. Chanhvongsak, and T. Stark, "A manufacturable chip-scale atomic clock," Transducers & Eurosensors, Lyon, France, 2007.
15. G. Alzetta, A. Gozzini, L. Moi, and G. Orriols, "Experimental-Method for Observation of Rf Transitions and Laser Beat Resonances in Oriented Na Vapor," Nuovo Cim. **36** (1), 5-20 (1976); E. Arimondo, in *Progress In Optics, Vol 35* (Elsevier Science Publ B V, Amsterdam, 1996), Vol. 35, pp. 257-354.
16. M. Zhu, "High contrast signal in a coherent population trapping based atomic frequency standard application," IEEE International Frequency Control Symposium and PDA Exhibition Jointly with the 17th European Frequency and Time Forum, Tampa, FL, 2003; M. Stähler, R. Wynands, S. Knappe, J. Kitching, L. Hollberg, A. Taichenachev, and V. Yudin, "Coherent population trapping resonances in thermal Rb-85 vapor: D-1 versus D-2 line excitation," Opt. Lett. **27** (16), 1472-1474 (2002).
17. Y. Y. Jau, E. Miron, A. B. Post, N. N. Kuzma, and W. Happer, "Push-pull optical pumping of pure superposition states," Phys. Rev. Lett. **93** (16), 160802 (2004); T. Zanon, S. Guerandel, E. de Clercq, D. Holleville, N. Dimarcq, and A. Clairon, "High Contrast Ramsey Fringes with Coherent-Population-Trapping Pulses in a Double Lambda Atomic System," Phys. Rev. Lett. **94** (19), 193002 (2005); V. Shah, S. Knappe, P.D.D. Schwindt, V. Gerginov, and J. Kitching, "Compact phase delay technique for increasing the amplitude of coherent population trapping resonances in open Λ systems," Opt. Lett. **31**, 2335-2337 (2006).
18. J. G. Coffler, M. Anderson, and J. C. Camparo, "Collisional dephasing and the reduction of laser phase-noise to amplitude-noise conversion in a resonant atomic vapor," Phys. Rev. A **65** (3 B), 033807 (2002).
19. P. R. Hemmer, D. P. Katz, J. Donoghue, M. Croningolomb, M. S. Shahriar, and P. Kumar, "Efficient Low-Intensity Optical-Phase Conjugation Based on Coherent Population Trapping in Sodium," Opt. Lett. **20** (9), 982-984 (1995); S. Babin, U. Hinze, E. Tiemann, and B. Wellegehausen, "Continuous resonant four-wave mixing in double- Lambda level configurations of Na₂," Opt. Lett. **21** (15), 1186-1188 (1996); A. Merriam, S. Sharpe, M. Shverdin, D. Manuszak, G. Y. Yin, and S. E. Harris, "Efficient Nonlinear Frequency Conversion in an All-Resonant Double- Λ System," Phys. Rev. Lett. **84** (23), 5308 - 5311 (2000); B. Lü, W. Burkett, and M. Xiao, "Nondegenerate four-wave mixing in a double-Lambda system under the influence of coherent population trapping," Opt. Lett. **23** (10), 804-806 (1998).
20. P. D. D. Schwindt, S. Knappe, V. Shah, L. Hollberg, J. Kitching, L. A. Liew, and J. Moreland, "Chip-scale atomic magnetometer," Appl. Phys. Lett. **85** (26), 6409-6411 (2004).
21. M. D. Eisaman, L. Childress, A. André, F. Massou, A. S. Zibrov, and M. D. Lukin, "Shaping Quantum Pulses of Light Via Coherent Atomic Memory," Phys. Rev. Lett. **93**, 233602 (2004).
22. C. Audoin, V. Candelier, and N. Dimarcq, "A limit to the frequency stability of passive frequency standards due to intermodulation effect," IEEE Trans. Instrum. Meas. **40** (2) (1991).
23. N. Vukičević, A. S. Zibrov, L. Hollberg, F. L. Walls, J. Kitching, and H. G. Robinson, "Compact diode-laser based rubidium frequency reference," IEEE Trans. UFFC **47** (5), 1122-1126 (2000); D. Strelakov, A. B. Matsko, N. Yu, A. A. Savchenkov, and L. Maleki, "Application of vertical cavity surface emitting lasers in self-oscillating atomic clocks," J. Mod. Opt. **53** (16-17), 2469-2484 (2006).
24. W. Demtröder, *Laser Spectroscopy*. (Springer, Berlin, 1996).
25. S. Knappe, V. Gerginov, P.D.D. Schwindt, V. Shah, H. Robinson, L. Hollberg, and J. Kitching, "Atomic vapor cells for chip-scale atomic clocks with improved long-term frequency stability," Opt. Lett. **30** (18), 2351-2353 (2005).